

Halogen-Free, Radiation-Curable, High-Refractive Index Materials

By Jeffrey Wang,
Marcus Hutchins,
Kenneth Woo, Toru Konish
and Mike J. Idacavage

High-refractive index (RI) materials, especially radiation-curable, high-RI materials, have been used in a wide variety of optical, photonic and electronic applications. Recently, there are fast-growing demands for new materials that offer even higher RI, higher performance and, especially, are halogen-free because of the increasing environmental concerns. Achieving equivalent RI without the use of halogenated materials, however, has been a major hurdle up until now. A unique, inorganic-organic hybrid nanocomposite technology platform has been developed which significantly improves nanoparticle compatibility with acrylated resins and, most important, minimizes viscosity increase. Unlike many nanoparticle dispersions which show various degrees of haziness because of particle agglomerations, this inorganic-organic hybrid nanocomposite technology demonstrates excellent optical transparency. Technical results from the newly developed high RI technologies, along with existing technologies for comparison purpose, will be discussed in this paper.

Introduction

The current trend is increasing demand for RI materials having high transparency and low birefringence for advanced integrated optical and optoelectronic applications.¹⁻³ Some

of the important and well-known applications include optical disks, diffraction gratings, optical fiber clad coatings, antireflection coatings, imaging sensors, light-emitting diodes (LED) and photonic devices such as waveguides and optical switches.⁴ High-refractive index coatings are applied to flat panel displays—such as liquid crystal displays (LCD)—as brightness-enhancing films (also known as a prism sheet). Polarizer films used in LCDs also require hard coatings with a high refractive index. High-refractive index coatings may improve the light emission and reception efficiency of white LEDs sufficiently to enable them to become the preferred light source of the 21st century. Antireflective films may improve the appearance of LCD and other display devices. Microlenses in charge-coupled devices (CCDs) made from high-refractive index materials may increase the amount of light received for higher sensitivity and higher definition. The creation of thin lenses will also contribute to the development of thinner equipment. Thus, there are many applications for high-refractive index materials.

In addition to pursuing higher refractive index and high optical transparency, depending upon features of the targeted applications, the chemist or material scientist must comprehensively keep all other requirements in mind. These

requirements include compatibility/solubility, processability, coatability and curability, along with the desired mechanical properties of surface hardness, toughness, elongation, coefficient of thermal expansion, photostability, thermal stability and proper adhesion to substrates.

Experimental Test Methods

Tensile strength (nominal) was calculated by dividing the maximum load by the original minimum cross-sectional area of the specimen according to ASTM D882-83. The result is expressed in force-per-unit area, usually MegaPascals (or pounds-force-per-square-inch).

Percent elongation at break was calculated by dividing the elongation at rupture by the initial length of the specimen and multiplying by 100. Gauge marks or extensometers are typically used to define a specific test section.

Elastic modulus was calculated by drawing a tangent to the initial linear portion of the load-extension curve, selecting any point on this tangent and dividing the tensile stress by the corresponding strain. For purposes of this determination, the tensile stress is calculated by dividing the load by the average original cross section of the test section. The result is expressed in force-per-unit-area, usually MegaPascals (or pounds-force-per-square-inch).

Pencil hardness was determined by a set of numbered pencils with varying degrees of hardness. The first pencil that scratches the surface is reported as the coating's hardness.

Viscosity measurements were obtained on a Brookfield DVII+ Viscometer using spindle #21 at a shear stress of 245-265 at 50-60% of full-scale reflection with a shear rate between 4 to 5 sec⁻¹ at 5 RPM. Sample readings were recorded after allowing chamber temperature to stabilize for 30 minutes and confirmed after another five minutes.

Particle size was determined using a Coulter brand LS230 Particle Size Analyzer. The instrument uses laser light scattering to detect particles in the range of 0.04 to 2,000 micrometers. Samples were fully dispersed in methanol after shaking for three minutes. Particle size data was collected and averaged more than 90 seconds for each run. The size calibration of the method was checked using reference standards at 15 and 55 micrometers.

Adhesion measurements were conducted according to ASTM D3359 method B (cross hatch) employing Permacel brand tape. The scale ranges from 5B (perfect adhesion) to 0B (greater than 65% adhesion loss).

The total UV dosage was 880 mJ/cm² under two (600 watt/inch) "H" doped lamps as measured by International Light's ILT 390C Belt Radiometer.

Results and Discussion

The refractive index (or index of refraction) of a medium is a measure for how much the speed of light (or other waves such as sound waves) is reduced inside the medium. The refractive index (*n*) of a medium

is defined as the ratio of the phase velocity (*c*) of a wave phenomenon such as light in a reference medium to the phase velocity (*V_p*) in the medium itself.

$$n = c / V_p \quad (1)$$

The Lorentz-Lorenz equation, which is also known as the Clausius-Mossotti relation and Maxwell's formula, relates the refractive index of a molecule/material to molar refractivity. After re-arrangement of the Lorentz-Lorenz equation, the refractive index (*n*) is given by:

$$n^2 = (8/3\pi N_A \gamma \rho + M) / (M - 4/3\pi N_A \gamma \rho) \quad (2)$$

where, *n* is the refractive index of molecule/material, *M* is the repeat unit of molecule, *N_A* is Avogadro's constant, *γ* is the polarizability and *ρ* is the density of molecule/material.

Equation 2 shows that the refractive index depends on the polarizability of the material; therefore, it is desirable to maximize the dipole moment-per-unit volume induced by the electromagnetic field. Substances containing more polarizable ("soft") groups (e.g., bromine, iodine, sulfur and phosphorus atoms or aromatic rings) or which have a high polarizability over a large atomic area will normally have higher refractive indexes than substances containing less polarizable ("hard") groups or than strongly electronegative substituents (such as fluorine, oxygen or alkyl groups) will have lower refractive indexes.^{5,6,7} As an example, see Table 1.⁸

TABLE 1

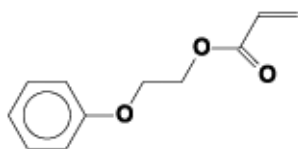
Effect of polarizable groups on refractive index

Substance	2-Iodoethanol	2-Fluoroethanol	Benzene	Cyclohexane
<i>n_D²⁰</i>	1.5720	1.3670	1.5010	1.4260

Based upon these theoretical considerations, four approaches to make high-refractive index materials have been identified:

1. Highly Aromatic Material

As discussed previously, bulky conjugated or aromatic substituents have a high refractive index. Therefore, a molecule that contains multiple aromatic rings may be expected to have an even higher refractive index. Bisphenol-A epoxy diacrylate has a refractive index of $n_D^{20} = 1.555$. While this product has a relatively high refractive index, its viscosity is relatively high, 800,000 cPs @ 25°C. It will be almost impossible to apply such a product by standard coating techniques. For this reason, a low-viscosity monomer with a single-ring structure was developed as shown below:



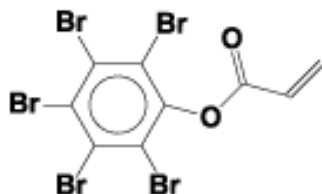
While having a relatively low-refractive index, $n_D^{20} = 1.516$, the monomer has low viscosity, 20 cPs @ 25°C, and good dilution capability.

Bisphenol-A epoxy diacrylate has a higher refractive index than the single-ring monomer does because the former contains two aromatic rings versus only one aromatic ring in the monomer. This suggests that increasing the number of aromatic rings is beneficial. However, if too many aromatic rings lay in the same plane within a molecule, birefringence can occur which may be problematic depending upon the application.

2. Highly Halogenated Material

Halogenation is a well-known approach to high-refractive index materials. A very typical halogenated molecule having a very high-refractive index (n_D^{20}) of 1.70 is pentabromophenyl methacrylate.

However, this molecule has a poor compatibility/solubility with other molecules because of its very high halogen content.

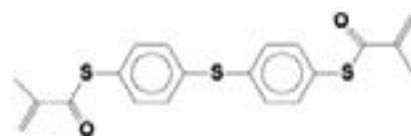


A brominated version of Bisphenol-A epoxy diacrylate has been developed which has a relatively high refractive index, $n_D^{20} = 1.588$ along with good compatibility with many other UV resins. Recently, there are globally fast-growing demands for only halogen-free materials with high refractive index because of the increasing environmental concerns. Achieving equivalent RI without the use of halogenated materials is a major challenge.

3. Heteroatom-Containing Material

Many conventional sulfur-containing molecules, particularly sulfur-containing aromatic molecules, are characterized by high optical transparency,⁹ high dielectric constant,¹⁰ good adhesion

to substrates¹⁰ and high refractive index.¹¹ One well-known example is bis(4-methacryloylthiophenyl) sulfide, or 4,4'-thiodibenzene dithiol dimethacrylate, which has very a high refractive index (n_D^{20}) of 1.66. However, it is in a solid state at room temperature and, more important, it has a very limited solubility/compatibility with other UV resins.



We have developed proprietary technologies that enable us to synthesize a series of heteroatom-containing aromatic urethane (meth)acrylate oligomers. These oligomers have a high refractive index, $n_D^{20} = 1.59 - 1.65$ (liquid), and excellent optical transparency. The oligomers typically have mono- or di(meth)acrylate functionality. Additionally, these oligomers are compatible with many commercial UV resins, thus making them easily formulated. Table 2 lists the properties of heteroatom-containing aromatic urethane (meth)acrylate oligomers, and Table 3 lists the performance of three formulations

TABLE 2

Two heteroatom aromatic urethane (meth)acrylate oligomers

Properties	Oligomer 1	Oligomer 2
Halogen-free	Yes	Yes
Appearance	Clear liquid	Deep brown, viscous liquid
Color (Gardner)	<1	<12.5
RI (L), n_D^{20}	1.606	1.639
Molecular weight (Mn) GPC	560	1,555
Viscosity (cP @ 60°C)	1,250	15,000
Density (g/cm ³)	1.18	1.19

TABLE 3

Performance data of formulations based on heteroatom aromatic urethane (meth) acrylate oligomer

	Formulation 1	Formulation 2	Formulation 3
Halogen-free	Yes	Yes	Yes
n_D^{20} (liquid)	1.5653	1.5658	1.5706
RI of cured film	1.5886	1.5883	1.5906
Viscosity at 25°C	1,840	1,290	5,500
Viscosity at 60°C	149	113	325
Pencil hardness	2H	1H	H
UV-cure dosage (mJ/cm ²)	880	880	880
Tensile, psi	2,700	2,039	2,337
Elongation, %	59	20	37
Modulus, psi	49,508	52,798	77,719
Toughness, psi	764	279	652
Adhesion to PET film, 5B=100% adhesion	5B	5B	5B

based on the heteroatom aromatic urethane (meth) acrylate oligomers.

3. Inorganic/Organic Hybrid Nanocomposite

Many inorganic materials are known to provide an extremely high refractive index. For examples, depending upon the types of crystal, TiO₂ may give a refractive index 2.4-2.6; ZrO₂ may provide a refractive index 2.0-2.4; ZnS has a refractive index 2.3; and ZnTe has a refractive index 3.5. However, they are complex and expensive to coat as they require methods such as vacuum-chemical vapor deposition.

Inorganic-organic hybrid composite materials have been proposed to obtain new types of materials with the combined advanced properties of both inorganic and organic materials. Particularly, for optical/optoelectronic applications, these hybrid composites are required to have highly optical clarity/transparence. Figure 1 presents

a photograph of three commercial nanoparticle dispersions that show significant light scattering. As shown, these nanoparticle dispersions are not useful for optical/optoelectronic applications.

The Rayleigh Scattering Equation^{12,13} describes the phenomenon of dispersion of electromagnetic radiation by particles that have a radius less than approximately 1/10 the wavelength of the radiation:

$$P_{scat.} = 128 \pi^5 N_0 r^6 / 3 \lambda^4 \cdot [(n_p^2 - n_m^2) / (n_p^2 + 2n_m^2)] \quad (3)$$

N₀: Avogadro constant,

r: particle radius, inorganic particle in this case,

λ: Wavelength of light,

n_p: RI of particles, RI of inorganic particle in this case,

n_m: RI of medium, RI of organic medium in this case

Where **P_{scat.}** is the total optical energy scattered by particles contained in matrix in all directions,

N₀ is Avogadro's constant, **r** is the particle radius, **λ** is the wavelength of the electromagnetic radiation, **n_p** is the refractive index of the particle, and **n_m** is the refractive index of the medium. Equation 3 shows that the intensity of scattered light increases significantly with increasing particle radius. The equation also shows that a larger difference between the RI of the inorganic particle and the RI of the organic medium gives higher intensity of scattered light. Of course, the intensity of scattered light is also closely related to the wavelength of light. For those inorganic-organic hybrid heterogeneous composite systems, in order to possess high optical transparency each individual phase has to be in a nano-scale, particularly, <50 nm, and preferably, <20 nm. Thus, controlling the particle size and the particle size distribution is absolutely critical. In addition, the refractive index difference between

FIGURE 1

Light scattering of nanoparticle dispersions



an inorganic phase and organic phase should be carefully managed.

Typically, inorganic-organic hybrid nanocomposites can be synthesized by two different methods—(1) sol-gel process and (2) nanoparticle dispersion in reactive organic medium.

In a sol-gel process, semimetal or metal alkoxides, chlorides or nitrates are hydrolyzed and then condensed. The sol-gel process uses a low processing temperature, which allows organic compounds to be homogeneously incorporated into inorganic structures without decomposition. In sol-gel systems, inorganic-organic hybrid coatings are crosslinked mainly by thermally induced MOH to MOH and MOH to M-OR, metal (or semimetal) alkoxide condensations, which generate highly crosslinked M-O-M networks with water or alcohol as byproducts. Unfortunately, neither hydrolysis nor condensation reactions can be completed unless high-temperature processes are used and this often decomposes the organic components or leads to cracking. It has been believed that composites produced by the sol-gel method exhibit unstable rheology and coatings formed from them may lack both thermal and hydrolytic stability. Such concerns have prevented

use of a large scale of such materials in commercial production.

Nanoparticle dispersion generally comprises inorganic fillers in nano-size, dispersed in organic components such as solvents, UV resins and/or polymers. However, the dispersions are prone to in-homogeneity, agglomeration and precipitation of inorganic fillers; thus improved stability and life time are highly desired.

A new technology for making nanocomposites with high refractive index which overcome some or all of the aforementioned problems has been developed. The new nanocomposite technology involves four features, including nanoparticle surface

modification, nanoparticle dispersion, nanocomposite stabilization and formulation of radiation (UV/EB)-curable, organic-inorganic hybrid nanocomposite.

Nanoparticle surface modification converts commercially-available nanoparticles that are hydrophilic and non-reactive to nanoparticles that are hydrophobic and curable.

Commercial nanoparticles are normally aqueous dispersions of inorganic oxides or metal particles. The average particle size is limited in the range of ≤ 20 nm, preferably ≤ 10 nm. The new technology utilizes proprietary coupling agents in nanoparticle surface modification reactions.

FIGURE 2

High-refractive index nanoparticle dispersion

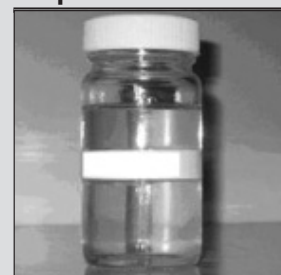


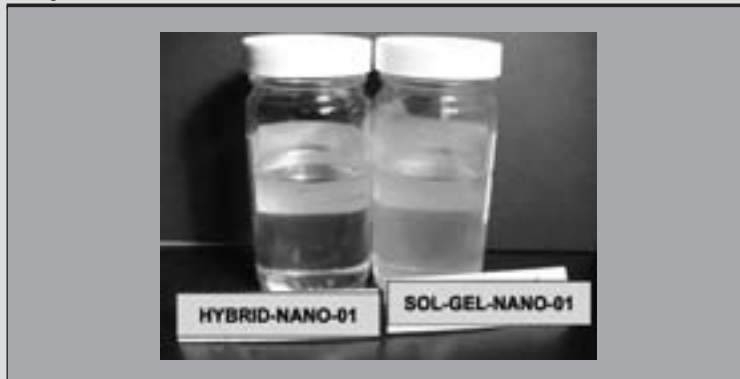
TABLE 4

Properties of high RI hybrid nanoparticle dispersion

High RI Nanoparticle Dispersion	Properties
Halogen-free	Yes
Organic medium	UV-resin
Appearance	Very light yellow, clear liquid
Color (Gardner)	<1
RI (L, 589 nm @ 25°C)	1.59
Viscosity (cP @ 25°C)	15,000
Density (g/cm ³)	1.26

FIGURE 3

Stability comparison of sol-gel nanoparticle dispersion (right) and hybrid nanoparticle dispersion (left)



After nanoparticle surface modification, the nanoparticles can be dispersed in desired UV resins and co-cured. This proprietary surface-treatment technology enables low viscosity, even at relatively high nanoparticle loadings and overcomes Rayleigh scattering issues for optical transparency (see Figure 2 and Table 4).

Also, a proprietary stabilization technology for preventing nanoparticle dispersion from agglomeration and precipitation of particles has been developed. This technology prevents changes (mainly increases) in the viscosity of the nanoparticle dispersion. In Figure 3, the sample SOL-GEL-NANO-01 is a nanoparticle dispersion made by the normal sol-gel process, while HYBRID-NANO-01 is a nanoparticle dispersion comprising a new surface treatment. With the same initial appearance (transparent liquid) for both samples, the sample SOL-GELNANO-01 became hazy and more viscous after 24 hours at room temperature. In contrast, HYBRID-NANO-01 remained almost unchanged under the same conditions. Figure 4 depicts the viscosity-time profile of SOL-GEL-NANO-02 and HYBRID-

NANO-02. One can see that the viscosity of HYBRID-NANO-02 did not significantly increase. In contrast, the viscosity of SOLGEL-NANO-02 continuously increased and finally gelled after aging for four weeks. HYBRIDNANO-02 can be considered thermally stable at 60°C.

As inorganic nanoparticles are surface-modified with organic groups, particularly as the surfaces

of nanoparticles are bonded with UV functional groups, the modified nanoparticles become compatible with various radiation-curable monomers and oligomers. Thus, a wide range of radiation-curable, inorganic-organic hybrid nanocomposites with high refractive index can be prepared. Note that all these nanocomposites are 100% reactive solids. Table 5 lists the performance data of a UV-curable, inorganic-organic, hybrid nanocomposite formulated based on one of the nanoparticle dispersions mentioned above. These results indicate that the nanocomposite provides excellent mechanical performance, particularly surface hardness.

Conclusions

Demands are growing faster for new materials which have even higher RI, higher performance and, especially, are halogen-free because of increasing environmental concerns. Achieving equivalent RI without the use of halogenated materials is a big challenge. Based on a broad understanding of the refractive

FIGURE 4

Comparison of viscosity changes as nanoparticle dispersion samples were aged at 60°C.

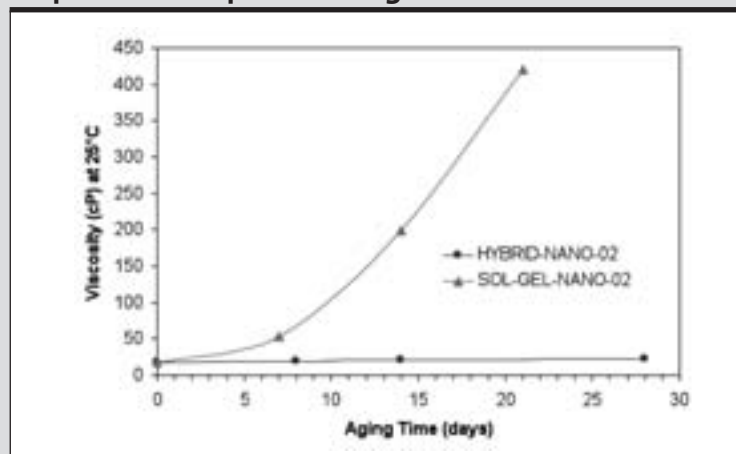


TABLE 5

Performance of a UV-curable, inorganic-organic hybrid nanocomposite formulation

Performance	Value
Halogen-free	Yes
Appearance	Clear liquid with yellow color
Color (Gardner)	<1
Density (g/cm ³)	1.24
n _D ²⁰ (liquid)	1.55
RI of cured film	1.58
Viscosity at 25°C	2,500
Viscosity at 60°C	100
Pencil hardness	5H
UV-cure dosage (mJ/cm ²)	880
Tensile, psi	4,000
Elongation, %	4.5
Tg°C (tan delta)	70
Toughness, psi	100
Adhesion to PET film, 5B=100% adhesion	5B

index, new technologies have now been developed which address this challenge, including heteroatom-containing materials and inorganic-organic, hybrid nanocomposites. The proprietary surface treatment of the nanomaterials results in dispersions with the high optical clarity required for optoelectronic applications. ■

References

- Nakamura, A.; Fujii, H.; Juni, N.; Tsutsumi, N. *Opt. Rev.* 2006, 13, 104.
- Mikami, A.; Koshiyama, T.; Tsubokawa, T. *Jpn. J. Appl. Phys.* 2005, 44, 608.
- Nakamura, T.; Tsutsumi, N.; Juni, N.; Fujii, H. *J. Appl. Phys.* 2005, 97, 054505.
- Jin-gang Liu,* Yasuhiro Nakamura, Yuji Shibusaki, Shinji Ando, and Mitsuru Ueda *Macromolecules* 2007, 40, 4614-4620
- Seferis, J.C., "Refractive Indices of Polymers" in *Polymer Handbook*, 4th ed., Brandrup, J. Immergut, E.H.; Grulke, E.A. Eds, Wiley: New York, 1999, VI, 571.
- Elias, H., "Plastics, General Survey" in *Ullmann's Encyclopedia of Industrial Chemistry*, 5th ed., Elvers, B.; Hawkins, S.; Schultz, G. Eds., VHS: New York, 1992, A20, 643.
- Pearson, J.M., "Vinyl Carbazole Polymers" in *Encyclopedia of Polymer Science and Engineering*, Wiley: New York, 1989, 257.
- The CRC Handbook of Chemistry and Physics.
- Matsuda, T.; Funae, Y.; Yoshida, M.; Yamamoto, T.; Takaya, T. *J. Appl. Polym. Sci.* 2000, 76, 50.
- Gaina, C.; Gaina, V. *Des. Monomers Polym.* 2005, 8, 347.
- Hirano, H.; Okada, T.; Nakamura, Y.; Kadota, J.; Watase, S.; Hasegawa, K. *Macromol. Mater. Eng.* 2006, 291, 205.
- Gao, C. Y.; Yang, B.; Shen, J. C. J. *J. Appl. Polym. Sci.* 2000, 75, 1474.
- B. M. Kerker "The Scattering of Light and Other Electromagnetic Radiation" Academic Press 1969, N.Y. & London.

—Jeffrey Wang, Marcus Hutchins, Kenneth Woo, Toru Konis and Mike J. Idacavage work in RADCURE™ Research & Development at Cytec Industries, Inc., in Smyrna, Ga.